



RESEARCH ARTICLE

Construction and characterization of two SARS-CoV-2 minigenome replicon systems

Hu Zhang^{1,2} | Douglas K. Fischer^{1,2} | Masahiro Shuda^{1,2} | Patrick S. Moore^{1,2} |
Shou-Jiang Gao^{1,2}  | Zandrea Ambrose^{1,2} | Haitao Guo^{1,2} 

¹Department of Microbiology and Molecular Genetics, University of Pittsburgh School of Medicine, Pittsburgh, Pennsylvania, USA

²Cancer Virology Program, Hillman Cancer Center, University of Pittsburgh Medical Center, Pittsburgh, Pennsylvania, USA

Correspondence

Haitao Guo, Department of Microbiology and Molecular Genetics, University of Pittsburgh School of Medicine, 5117 Centre Ave, Pittsburgh, PA 15213, USA.
Email: guoh4@upmc.edu

Funding information

UPMC Hillman Cancer Center; Pittsburgh Foundation; Clinical and Translational Science Institute, University of Pittsburgh; DSF Charitable Foundation

Abstract

The ongoing COVID-19 pandemic severely impacts global public health and economies. To facilitate research on severe acute respiratory syndrome coronavirus 2 (SARS-CoV-2) virology and antiviral discovery, a noninfectious viral replicon system operating under biosafety level 2 containment is warranted. We report herein the construction and characterization of two SARS-CoV-2 minigenome replicon systems. First, we constructed the IVT-CoV2-Rep complementary DNA template to generate a replicon messenger RNA (mRNA) with nanoluciferase (NLuc) reporter via in vitro transcription (IVT). The replicon mRNA transfection assay demonstrated a rapid and transient replication of IVT-CoV2-Rep in a variety of cell lines, which could be completely abolished by known SARS-CoV-2 replication inhibitors. Our data also suggest that the transient phenotype of IVT-CoV2-Rep is not due to host innate antiviral responses. In addition, we have developed a DNA-launched replicon BAC-CoV2-Rep, which supports the in-cell transcription of a replicon mRNA as initial replication template. The BAC-CoV2-Rep transient transfection system exhibited a much stronger and longer replicon signal compared to the IVT-CoV2-Rep version. We also found that a portion of the NLuc reporter signal was derived from the spliced BAC-CoV2-Rep mRNA and was resistant to antiviral treatment, especially during the early phase after transfection. In summary, the established SARS-CoV-2 transient replicon systems are suitable for basic and antiviral research, and hold promise for stable replicon cell line development with further optimization.

KEYWORDS

antiviral agents, cellular effect, disease control, immune responses, innate immunity, mRNA/splicing, SARS coronavirus, virus classification

1 | INTRODUCTION

The ongoing COVID-19 pandemic, which first broke out in Wuhan, China, in December 2019,^{1,2} has affected over 310 million people and caused over 5.5 million deaths worldwide as of January 15, 2022 according to the World Health Organization (<https://covid19.who.int/>). The disease is caused by infection with the severe acute respiratory syndrome coronavirus 2 (SARS2-CoV-2).³ Vaccines and

antiviral agents are urgently needed to mitigate and end the pandemic. Despite the development and application of SARS-CoV-2 vaccines, the rapid evolution of viral spike (S) protein and emergence of many variants of concern have often resulted in vaccine breakthrough cases and caused new waves of infections.^{4,5}

SARS-CoV-2 is an enveloped, positive-sense RNA virus, belonging to the *Coronaviridae* family. The virus possesses a large RNA genome of ~30 kb in length, with a genome organization similar to

previously characterized coronaviruses (Figure 1).^{6,7} Approximately two-thirds of the viral genome encodes an open reading frame (ORF), ORF1ab, which is the only ORF directly translated into proteins from the full-length viral genome. ORF1ab is translated into two polypeptides, specifically PP1a and PP1ab, via a programmed -1 ribosome frameshift mechanism.⁸ The polypeptides undergo autoproteolysis to release a number of nonstructural proteins (NSPs) including proteases, RNA-dependent RNA polymerase (RdRp, also known as NSP12), as well as other NSPs required for viral RNA replication and transcription.⁹ The translated replicase and transcriptase proteins engage the viral genome to assemble the replicase-transcriptase complex (RTC) on endoplasmic reticulum membrane, forming a membranous compartment.¹⁰ Within the membranous

compartment, the RTC completes viral replication and transcription. The latter involves a transcription regulatory sequences (TRS)-mediated discontinuous RNA synthesis, which results in that all the viral transcripts contain the same 5'-leader and 3'-terminal sequences from the full-length genome.^{11,12} Transcription of the 3'-terminal genome by viral RTC generates a nested set of subgenomic messenger RNAs (mRNAs) that encode structural proteins and accessory genes. Viral structural proteins include the spike (S), membrane (M), envelop (E), and nucleocapsid (N) proteins required for virion assembly.¹³

Establishing SARS-CoV-2 infection and/or replication systems in the laboratory setting is indispensable for basic and antiviral research. Reverse genetics represents a powerful approach

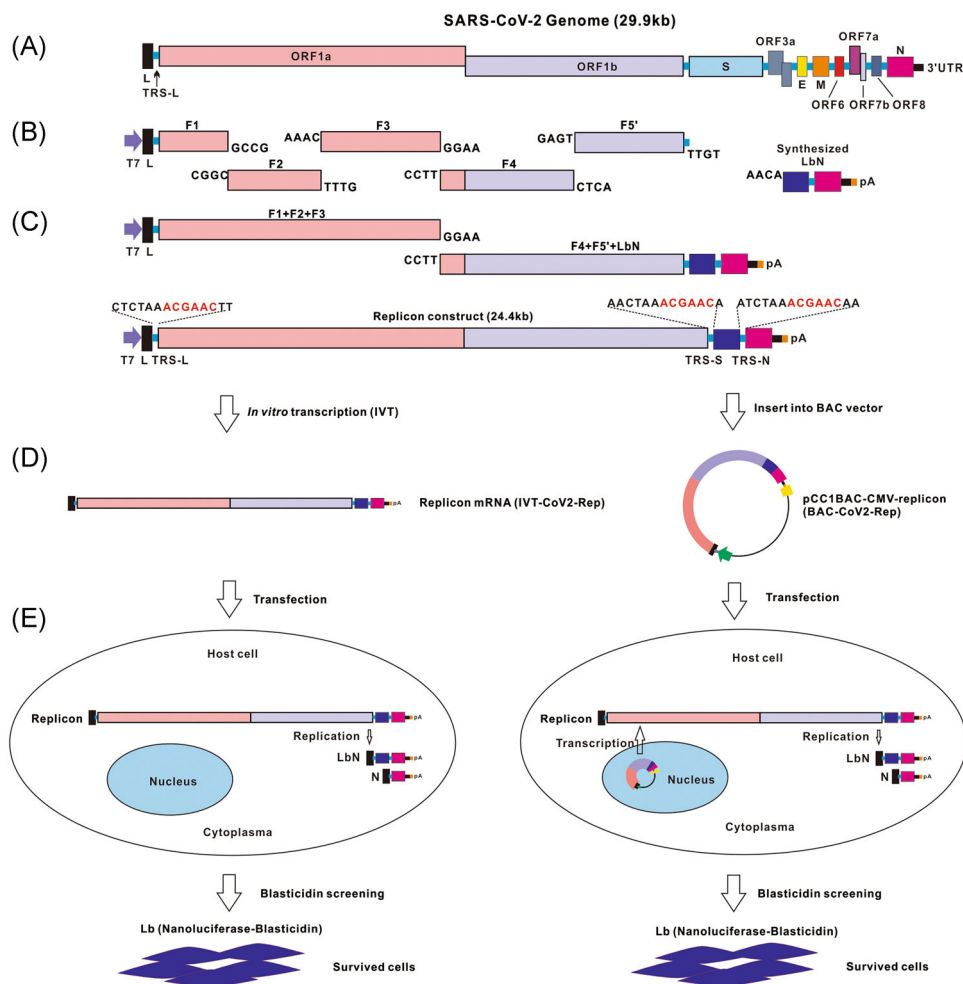


FIGURE 1 Schematic design of SARS-CoV-2 minigenome replicons. (A) The genome organization of SARS-CoV-2 is schematically presented with the major ORFs indicated as color blocks. (B) The synthesized DNA fragments of ORF1ab (F1'-F5') and LbN cassette are shown with their ligatable cohesive ends. The T7 promoter sequence and a poly(A) tail are located at the 5' terminus of F1 and 3' terminus of LbN, respectively. (C) The DNA fragments are directionally ligated in vitro to assemble the IVT-CoV2-Rep cDNA. The nucleotides shown above the blue boxes are site-specific viral transcription regulatory sequences (TRS). (D) IVT-CoV2-Rep cDNA serves as an IVT template to synthesize replicon mRNA or it is cloned into pCC1BAC-CMV-PreSARS2 vector to construct BAC-CoV2-Rep. (E) IVT-CoV2-Rep mRNA or BAC-CoV-Rep is transfected into mammalian cells for assessment of replicon replication and stable replicon cell line selection. See text for more details. BAC, bacterial artificial chromosome; cDNA, complementary DNA; CMV, cytomegalovirus; IVT, in vitro transcription; E, envelope gene; L, leader sequence; Lb, nanoluciferase (NLuc)-blasticidin S-resistance (BSR) fusion gene; M, membrane protein; mRNA, messenger RNA; N, nucleocapsid gene; ORF, open reading frame; S, spike gene; SARS-CoV-2, severe acute respiratory syndrome coronavirus 2

for this purpose, by which recombinant viruses are engineered to express reporter genes to facilitate antiviral drug screening, and attenuated viruses or viral replicons can be generated to provide a safer biocontainment environment for studying potentially lethal infectious viruses.^{14,15} Self-amplifying viral replicon RNA systems that recapitulate the core events of intracellular viral genome synthesis, but avoid the production of infectious viral particles, have been successfully utilized in virus research and antiviral drug discovery, as exemplified by the hepatitis C virus (HCV) replicon.^{16,17} Previous studies have used various approaches to assemble coronavirus replicons. Some made use of *in vitro* ligation to assemble the replicon complementary DNA (cDNA), followed by *in vitro* transcription (IVT) to generate replicon mRNA^{18–21}; others used transformation associated recombination (TAR) or a bacterial artificial chromosome (BAC) to assemble replicon cDNA and then produce replicon mRNA by IVT.^{22,23} The IVT mRNA were then transfected into target host cells to initiate replicon RNA replication. While these IVT RNA-based approaches have been demonstrated to work, they also face the technical challenge of producing full-length viral RNA of ~25 kb, especially when scale-up production is required. For example, instead of full-length RNA, shorter RNA species have been shown to be the major transcripts produced by IVT of replicon cDNA.^{20,24} A recent study reported a DNA-launched BAC system that appeared to be an effective and simple approach to generate SARS-CoV-2 replicon RNA with high signal; however, this system was refractory to antiviral drug treatment.²⁵ Furthermore, for unknown reasons, all the reported SARS-CoV-2 replicon RNA systems were transient in cells, and a stable replicon cell line has not been established so far.

Here, we report our work on SARS-CoV-2 minigenome replicon construction and optimization. First, we used the prokaryotic T7 promoter-driven IVT to generate IVT-CoV2-Rep mRNA with a nanoluciferase (NLuc) reporter from the replicon cDNA, followed by cell transfection. The experimental results demonstrated that IVT-CoV2-Rep worked in a variety of host cell lines. Although the replicon signal was low and transient for several days, it could be completely abolished by known SARS-CoV-2 protease and RdRp inhibitors. Furthermore, our data suggested that the transient phenotype of IVT-CoV2-Rep was unlikely due to host innate antiviral responses. In addition, we have also developed a BAC plasmid-based replicon (BAC-CoV2-Rep), which supports the transcription of full-length replicon mRNA under the control of a eukaryotic cytomegalovirus-immediate early (CMV-IE) promoter upon transfection into host cells. The BAC-CoV2-Rep system exhibited a much stronger and longer replicon signal compared to the IVT-CoV2-Rep version. We also found that a portion of the BAC-CoV2-Rep NLuc reporter signal was derived from spliced replicon mRNA and resistant to antiviral treatment, especially during the early phase after transfection. Taken together, the BAC-CoV2-Rep system holds promise for basic and antiviral research, as well as stable replicon cell line development with further optimization.

2 | MATERIALS AND METHODS

2.1 | Cell lines

The African green monkey kidney epithelial cell line Vero, Chinese hamster ovary cell line CHO-K1, and baby hamster kidney cell line BHK-21, were purchased from the American Type Culture Collection. The human hepatoma cell line Huh7.5 was kindly provided by Dr. Charles Rice (Rockefeller University).²⁶ The human lung epithelial cell line A549DKO with protein kinase R (PKR) and ribonuclease L (RNase L) double knockout was kindly provided by Dr. Bernard Moss (National Institute of Allergy and Infectious Diseases/National Institutes of Health [NIAID/NIH]).²⁷ Cells were maintained in Dulbecco's modified Eagle's medium:nutrient mixture F-12 supplemented with 10% fetal bovine serum and 1% penicillin/streptomycin.

2.2 | Construction of SARS-CoV-2 minigenome replicons

As illustrated in Figure 1, the 5'-portion of SARS-CoV-2 genome (Isolate USA_WA1/2020) was split into multiple cDNA fragments. The cDNA fragment-containing plasmids pUC57-F1, pCC1BAC-F2, pCC1BAC-F3, and pUC57-F4 were kindly provided by Dr. Pei-Yong Shi (University of Texas Medical Branch).²⁴ SARS-CoV-2 genomic RNA (NR-52285, Isolate USA_WA1/2020) was obtained from the BEI Resources Program supported by NIH/NIAID and a kind gift of Dr. Paul Duprex (University of Pittsburgh Center for Vaccine Research), and cDNA was synthesized from 100 ng of the SARS-CoV2 RNA by iScript cDNA Synthesis Kit (BioRad). The F5' fragment was amplified from the cDNA of SARS-CoV-2 mRNA by Q5 high-fidelity polymerase chain reaction (PCR) using the primers indicated in Table S1. The 5' ends of F5' forward and reverse primers were designed to contain the Type IIS restriction enzyme Esp3I site. The TRS element before S ORF (TRS-S) in SARS-CoV2 genome was included in the reverse primer (F5'r). The F5' PCR fragment was cloned into pSC-A-amp kan (Agilent) vector to obtain plasmid pSC-A-F5'. Plasmid pUAS-NanoLuc expressing NLuc was a gift from Dr. Robert Campbell (Addgene plasmid # 87696).²⁸ The LbN DNA fragment containing the NLuc and blasticidin S-resistance gene (BSR) fusion gene ORF (Lb) and SARS-CoV-2 N ORF in tandem was partially synthesized by Genscript and assembled with a NLuc-containing PCR fragment amplified from pUAS-NanoLuc. An 85-nt sequence containing TRS-N upstream of N ORF was included in LbN. A poly(A) tail of 33 nt was placed at the 3' terminus of LbN. The Esp3I site was introduced to the 5' and 3' termini of LbN as well. LbN fragment was subcloned into pcDNA3.1/V5-His (V81020; Invitrogen) to obtain pcDNA3.1-LbN. Plasmid pcDNA6B-N expressing the C-terminally FLAG-tagged SARS-CoV-2 N protein was a gift from Dr. Pei-Hui Wang (Shandong University) and Dr. Yuan Liu (Cornell University).²⁹ All fragments were sequenced and confirmed to be correct according to the SARS-CoV-2 full-length genome reference sequence (NCBI GenBank accession number: NC_045512).

F1, F2, F3, and F4 cDNA fragments were acquired by BsaI digestion and F5' and LbN fragments were obtained by Esp3I digestion from their corresponding plasmids. The restricted fragments were resolved in a 0.8% agarose gel and purified using the QIAquick Gel Extraction Kit (Qiagen). The full-length IVT-CoV2-Rep cDNA was generated by in vitro ligation of the six contiguous panel of cDNA with T4 DNA ligase (NEB).

To construct BAC-CoV2-Rep, the full-length IVT-CoV2-Rep cDNA was inserted into an engineered pCC1BAC-CMV-PreSARS2 vector, in which the CMV-IE promoter and a portion of the 5'-leader and 3' terminal sequence of SARS-CoV-2 genome were inserted into a commercially available vector pCC1BAC (Epicentre). BsiWI and XhoI double digestion was conducted to create the cohesive ends for IVT-CoV2-Rep and pCC1BAC-CMV-PreSARS2, followed by DNA ligation of the purified target DNA fragments and transformation into TransforMax EPI300 (Lucigen) competent cells. The pCC1BAC is a copy-control plasmid. EPI300 *Escherichia coli* contains an inducible *trfA* gene, whose protein product is required for initiation of replication from *oriV*, the replication origin of pCC1BAC.³⁰ When no induction solution is added, the bacteria maintains one copy of pCC1BAC plasmid per cell and thus maintains the stability of the long exogenous DNA insert. When high copies of pCC1BAC plasmid are needed for transfection, the induction solution is added into the bacterial culture per the manufacturer's instructions. BsiWI and XhoI double digestion was used for screening the positive clones of BAC-CoV2-Rep.

2.3 | In vitro transcription

The IVT-CoV2-Rep mRNA was in vitro transcribed by the mMES-SAGE mMACHINE T7 Transcription Kit (Thermo Fisher Scientific) according to the manufacturer's instruction with minor modifications. One microgram of IVT-CoV2-Rep cDNA was subjected to IVT. Cap analog to GTP ratio was set to 1:1. The reaction was incubated overnight at 30°C. After removal of DNA template by RQ1 RNase-Free DNase treatment, RNA was precipitated by LiCl. Pelleted RNA was washed once with 70% ethanol, dried by air and dissolved in 30 μ l diethylpyrocarbonate-treated water. The purified RNA samples were quantified by Nanodrop spectrophotometer (Thermo Fisher Scientific) and subjected to native and denature agarose gel electrophoresis for quality assessment.

The EcoRV-linearized pcDNA3.1-LbN and XbaI-linearized pcDNA6B-N were used as IVT templates for LbN and N mRNA transcription, respectively, as above described except that the IVT reaction time was reduced to 1 h.

2.4 | Northern blot

To prepare the riboprobe targeting the F1 fragment region of full-length SARS-CoV-2 replicon mRNA, a pair of PCR primers, specifically probeF1f and SP6probeF1r (Table S1), were used to amplify the

DNA template from pUC57-F1. The purified PCR product served as the template for SP6 IVT (P1420; Promega) of the radiolabeled F1 riboprobe in the following reaction mixture: 2 μ l of purified F1 riboprobe DNA template (500 ng/ μ l), 4 μ l of transcription optimized 5X buffer, 2 μ l of 100 mM DTT, 1 μ l of RNase inhibitor (20 units/ μ l), 4 μ l of rATP, rGTP, rCTP, and UTP mix (2.5 mM each except for 0.125 mM of UTP), 1 μ l of SP6 RNA polymerase (20 units/ μ l), and 6 μ l of [³²P]-UTP (10 mCi/ml; PerkinElmer). After incubation of the reaction at 37°C for 1 h, 1 μ l of RQ1 RNase-free DNase (1 U/ μ l) was added to remove the DNA template, and the riboprobe was purified and the radioactivity was measured by a scintillation counter (PerkinElmer) according to our published protocol.³¹ To make the riboprobe targeting the N gene sequence in all the full-length and subgenomic mRNAs of SARS-CoV-2, a 123-bp PCR product amplified by the N gene qPCR primers (Table S1) was inserted into pGEM-T Easy vector (Promega) to generate pGEM-T-N, in which the antisense sequence of N is in the same orientation as the SP6 promoter carried by the vector. The NcoI-linearized pGEM-T-N was used as the template for IVT of N riboprobe as described above.

RNA samples were resolved in a 0.8% agarose gel containing 2.2 M formaldehyde and transferred onto Hybond-XL membrane (GE Healthcare) in 20X saline sodium citrate (SSC) buffer. Membranes were hybridized with the aforementioned F1 or N riboprobe in 5 ml EKONO hybridization buffer (G-Biosciences) with 1 h prehybridization at 65°C and overnight hybridization at 65°C, followed by a 1-h wash with 0.1X SSC and 0.1% sodium dodecyl sulfate at 65°C. The membrane was exposed to a phosphorimager screen and the hybridization signals were scanned by the Typhoon FLA-7000 imager (GE Healthcare) and quantified by QuantityOne (Bio-Rad).

2.5 | Reverse transcription-quantitative PCR and reverse transcription-PCR

For reverse transcription-quantitative PCR (RT-qPCR) of IVT-CoV2-Rep RNA, the cDNA templates were prepared with 10 ng input RNA, F1-specific RT primer (Table S1, 1 μ M final concentration) or oligo (dT) (2.5 μ M final concentration) by using Transcriptor First Strand cDNA Synthesis Kit (Roche). The qPCR reaction was assembled as follows: 10 μ l of 2X Roche LightCycler 480 SYBR Green I Master Mix, 0.5 μ l of each forward and reverse primer (Table S1, 20 μ M stock), and 2 μ l RT product in a total volume of 20 μ l. The qPCR was run on Roche LightCycler 96 with the following program: Preincubation 95°C 5 min, 45 cycles amplification (95°C 10 s, 55°C 20 s, and 72°C 20 s at single acquisition mode), and then followed by a melting curve step (95°C 5 s, 65°C 1 min, and 97°C 10 acquisitions at continuous acquisition mode). Serially diluted plasmid pUC57-F1 and pcDNA3.1-LbN were used to generate qPCR standard curves for quantitation.

The RT-qPCR and RT-PCR of interferon (IFN)- β and glyceraldehyde 3-phosphate dehydrogenase (GAPDH) mRNA from CHO-K1 cells were performed using gene-specific primers listed in Table S1.

RT-PCR of total RNA extracted from BAC-CoV2-Rep-transfected cells was conducted using splicing-specific RT and PCR primers (Table S1). The RT-PCR products were resolved in an agarose gel and the visualized DNA bands were purified and cloned into the pSC-A-amp/kan vector (Agilent) for Sanger sequencing.

2.6 | Replicon transfection and NLuc quantification

IVT-CoV2-Rep mRNA was transfected into mammalian cells by using Lipofectamine MessengerMAX Transfection Reagent (Invitrogen) at a 1:2 ratio ($\mu\text{g}:\mu\text{l}$). Alternatively, the mRNA was transfected into cells by Gene Pulser Xcell Electroporation Systems (Bio-Rad) using the preset protocols on the instrument. Plasmid BAC-CoV2-Rep was transfected into cells using Lipofectamine 3000 (Invitrogen). At indicated time points post-transfection, cells were lysed with Nano-Glo NLuc solution (N1120; Promega) and the luminescence signal was detected using a Synergy HTX Microplate Reader (BioTek).

2.7 | Immunofluorescence assay

The transfected cells were fixed with 4% paraformaldehyde, followed by permeabilization with 0.5% Triton-X. After blocking with normal immunofluorescence assay buffer (10% fetal bovine serum + 2% bovine serum albumin in phosphate-buffered saline solution), the cells were first incubated with primary antibodies against SARS-CoV-2 N protein (40143-MM05; Sinobiological), followed by incubation with fluorescence-labeled secondary antibodies. The cells were mounted in a mounting medium containing 4',6-diamidino-2-phenylindole. Fluorescence images were acquired by a fluorescence microscope (EVOS M5000; Thermo Fisher Scientific).

2.8 | Compounds

SARS-CoV-2 antiviral compounds remdesivir, GC376, and EIDD-1931 were purchased from SelleckChem. Remdesivir and GC376 were dissolved in dimethyl sulfoxide (DMSO) to make 10 mM stocks. EIDD-1931 was dissolved in water to make a 10 mM stock. RIG-I ligand 5' triphosphate hairpin RNA (3p-hpRNA) was purchased from InvivoGen. PKR inhibitor C16 was purchased from Bio-Techne.

2.9 | Statistical analysis

Data are provided as the mean \pm standard deviation. Calculations and graphs were generated using GraphPad Prism 9.0. Student's *t* test was used to determine the statistical significance. A *p* value less than 0.05 ($p < 0.05$) was considered statistically significant.

3 | RESULTS

3.1 | The construction of SARS-CoV-2 replicons

The workflow of our design of the SARS-CoV-2 replicons is schematically illustrated in Figure 1. The designed minigenome replicon contains the viral NSP genes (ORF1a and ORF1b) and the N gene required for coronavirus RNA replication.³² The cluster of viral structural protein genes (S, E, and M) and accessory proteins genes between ORF1ab and N are excluded to avoid production of infectious virus and to minimize the size of the replicon. To facilitate the detection of replicon replication and selection of replicon-positive cell clones, the NLuc and BSR fusion gene Lb is inserted between ORF1b and N. The viral TRS-S ORF is linked to the 5' end of Lb gene for transcription of LbN mRNA during replicon replication. The design of LbN mRNA-dependent NLuc expression was validated by transfection of pcDNA3.1-LbN or LbN IVT mRNA into cells (Figure S1). A T7 promoter sequence is placed at the 5' end of the replicon cDNA for IVT of replicon mRNA (IVT-CoV2-Rep). As an alternative approach, the IVT-CoV2-Rep cDNA is cloned into p1CCBAC-CMV-PreSARS2 vector to generate BAC-CoV2-Rep, which serves as template to initiate intracellular transcription of replicon mRNA upon transfection.

We took an *in vitro* ligation strategy to assemble the IVT-CoV2-Rep cDNA (Figure 2). Fragments F1-F4 were released by BsaI digestion and F5' and LbN were acquired by Esp3I digestion from their corresponding plasmids (Figure 2A). The digested target fragments with ligatable cohesive ends were gel purified and validated by electrophoresis (Figure 2B). To optimize the outcome of *in vitro* ligation, we first did F1 + F2 ligation and F4 + F5' ligation, respectively. Then, F3 was added to F1 + F2 ligation and LbN was added to F4 + F5' ligation. Finally, the F1 + F2 + F3 and F4 + F5' + LbN ligation reactions were mixed together to obtain the full-length IVT-CoV2-Rep cDNA of 24.4 kb, although intermediate ligation products could also be seen (Figure 2C).

Then, the IVT-CoV2-Rep cDNA was subjected to T7 promoter-mediated IVT. The IVT products exhibited a predominant species around 1.5 kb with a long smear in a native agarose gel electrophoresis (Figure 2D). We also ran the IVT products in a denaturing gel and conducted Northern blotting using riboprobes targeting the N ORF and the F1 region, respectively (Figure S2). A strong hybridization signal at a low molecular weight position was detected by the F1 probe but not the N probe, which was likely the nascent IVT products. However, full-length replicon RNA was not detected by either the F1 or the N riboprobes, indicating that the IVT of full-length replicon mRNA was inefficient likely due to the large size of the IVT-CoV2-Rep cDNA template. To examine whether the full-length replicon RNA was produced by IVT, we developed a more sensitive RT-qPCR assay to detect the F1 and N region, respectively (Table S1, Figures S3 and S4). According to the IVT-CoV2-Rep design (Figure 1), while the F1-specific RT-qPCR should detect the full-length replicon RNA and the majority of immature IVT products, the oligo(dT)/N-specific RT-qPCR should only detect full-length RNA. The results demonstrated that the full-length IVT-CoV2-Rep mRNA was indeed

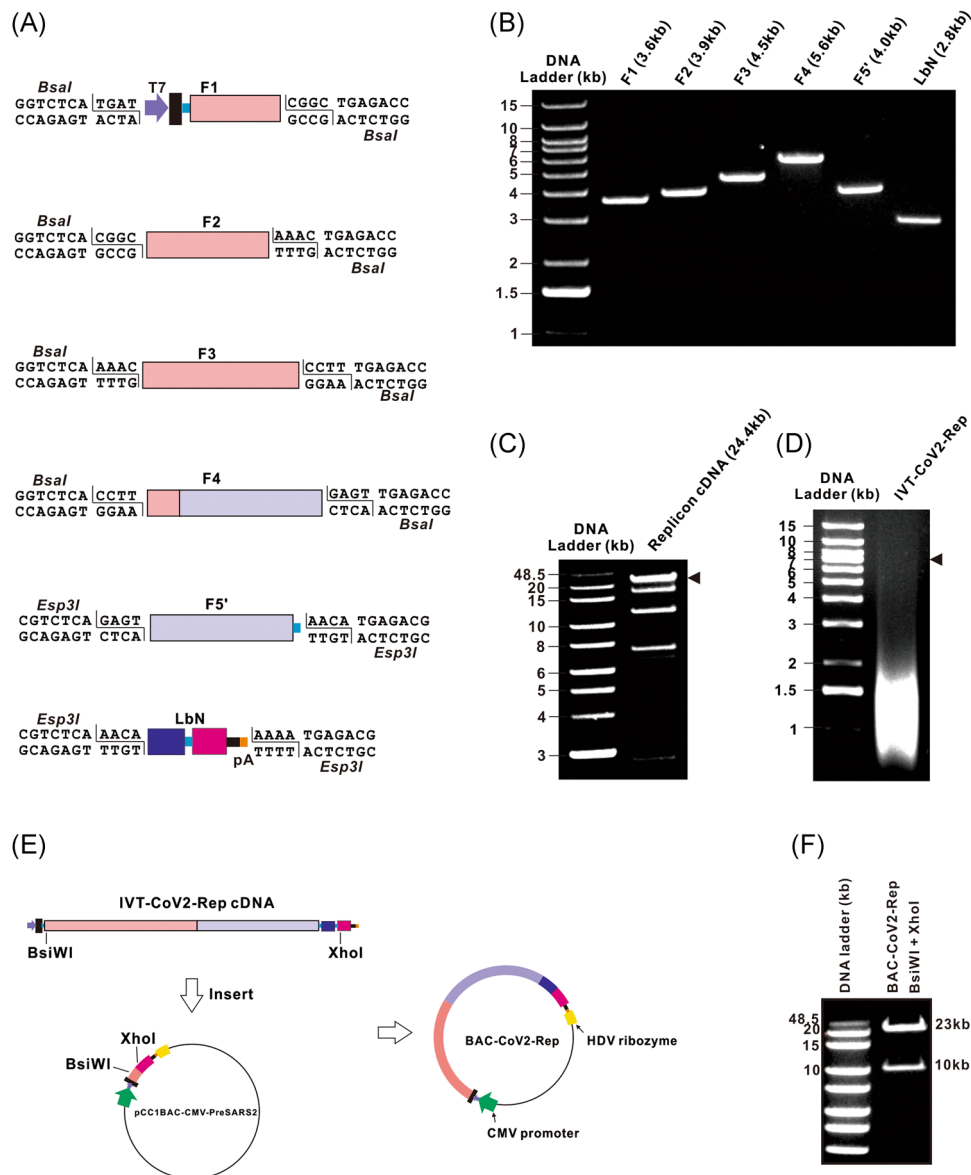


FIGURE 2 Assembly of SARS-CoV-2 replicons. (A) A diagram of each cDNA fragment with the terminal *Bsal* or *Esp3I* restriction site is shown. (B) Gel analysis of the purified cDNA fragments is presented. The individual cDNA fragments (F1 to LbN) were released from corresponding plasmids by *Bsal* or *Esp3I* as indicated in (A) and gel purified, followed by purity examination on a 0.8% agarose gel. A 1 kb plus DNA ladder served as size marker. (C) Gel analysis of the cDNA ligation products is shown. 1 μ g of purified ligation product was analyzed on a 0.8% agarose gel. The triangle indicates the full-length IVT-CoV2-Rep cDNA product. (D) Gel analysis of IVT RNA transcripts is shown. 1 μ g of IVT-CoV2-Rep RNA was analyzed on a 0.8% native agarose gel. Note that the DNA size markers do not directly correlate with the RNA size. The triangle indicates the approximate position of the full-length replicon transcript. (E) The strategy of construction of BAC-CoV2-Rep is shown. The assembled IVT-CoV2-Rep cDNA was digested by *BsiWI*/*XhoI* and inserted into the corresponding restriction site of pCC1BAC-CMV-PreSARS2 to generate BAC-CoV2-Rep. The CMV promoter and HDV ribozyme site carried by the vector backbone are indicated. (F) The positive clone of BAC-CoV2-Rep was verified by *BsiWI*/*XhoI* double digestion and analysis by agarose gel electrophoresis. BAC, bacterial artificial chromosome; cDNA, complementary DNA; CMV, cytomegalovirus; HDV, hepatitis delta virus; IVT, in vitro transcription; SARS-CoV-2, severe acute respiratory syndrome coronavirus 2

produced by IVT, although it only comprised approximately 1% of the total IVT products (Table S2).

To construct BAC-CoV2-Rep, we took advantage of the unique *BsiWI* and *XhoI* restriction sites located in the 5' F1 region and 3' N ORF in the IVT-CoV2-Rep construct, respectively. The acceptor plasmid pCC1BAC-CMV-PreSARS2 harbors the tandem CMV-IE and

T7 promoters, a portion of the 5' and 3' terminal sequence of SARS-CoV2 genome, and the hepatitis delta virus ribozyme sequence (Figure 2E). Therefore, the *BsiWI*/*XhoI*-restricted fragment from IVT-CoV2-Rep cDNA was cloned into the corresponding site in the pCC1BAC-CMV-PreSARS2 vector. The positive BAC-CoV2-Rep clone was verified by *BsiWI*/*XhoI* double digestion (Figure 2F).

3.2 | Characterization of IVT-CoV2-Rep

The IVT-CoV2-Rep mRNA or N mRNA IVT product was transfected into various cell lines, including Vero, CHO-K1, Huh7.5, and BHK-21. The replicon RNA replication was assessed by measuring NLuc activity in transfected cells. The transfection of the replicon mRNA resulted in increased NLuc signal compared to control N mRNA transfection (Figure 3A–D). On the basis of principle of coronavirus genome replication and our replicon design, the NLuc activity encoded by the Lb fusion protein is an indicator of sub-genomic LbN mRNA expression (Figure 1). Thus, the appearance of NLuc activity suggested that IVT-CoV2-Rep replication took place successfully in transfected cells. Among the different cell lines transfected with IVT-CoV2-Rep mRNA, NLuc activity was highest in CHO-K1. The NLuc activity in Vero, CHO-K1, and Huh7.5 cells peaked at 2 days posttransfection (Figure 3A–C). In BHK-21 cells, the NLuc activity peaked at 4 days posttransfection (Figure 3D). We repeated the above experiments multiple times and found that the peak time of NLuc activity varied between 1 and 4 days after replicon mRNA transfection, likely due to the variabilities in cell culture and/or other experimental conditions. However, in most instances, the NLuc activity peaked at Day 1–2 posttransfection, followed by significant decline, in a 5-day course of experiment (data not shown).

We then checked whether the observed transient replicon replication could rebound in a prolonged culture of transfected cells. We chose CHO-K1 and BHK-21 cells for further study based on the relatively higher replicon-NLuc activity produced in these two cell lines. As shown in Figure 3E,F, THE NLuc activity peaked early but quickly declined to background level within 4 days posttransfection, and remained at background level over 5 days of additional follow-up monitoring, indicating the presence of a quenching host antiviral mechanism(s) or lack of a viral factor(s) responsible for the observed transient phenotype of IVT-CoV2-Rep.

3.3 | IVT-CoV2-Rep is sensitive to antiviral inhibitors

Next, we tested the sensitivity of IVT-CoV2-Rep to several known SARS-CoV-2 replication inhibitors, including Remdesivir, GC376, and EIDD-1931. Remdesivir and EIDD-1931 are nucleoside RdRp inhibitors,^{33,34} and GC376 is a 3C-like protease inhibitor.³⁵ Since remdesivir and GC376 are soluble in DMSO but not in water, while EIDD-1931 is soluble in water but not in DMSO, both DMSO and water were used as solvent controls. We first assessed the potential influence to replicon assay in different solvents and found that DMSO could reduce the replicon-derived NLuc activity by ~10-fold

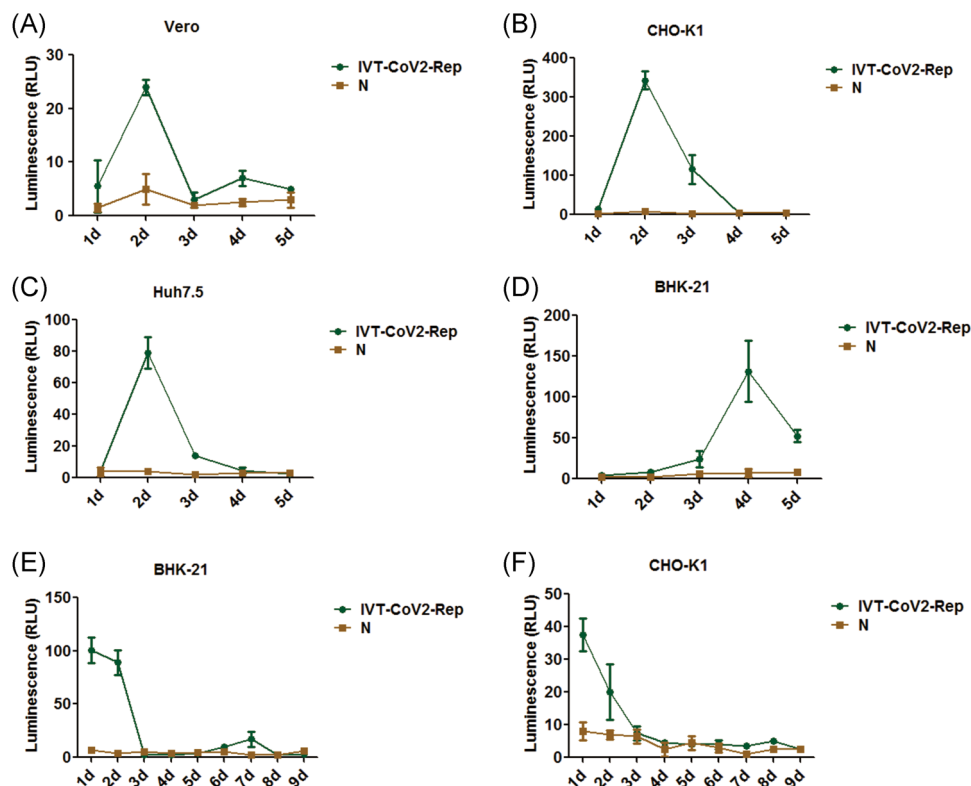


Figure 3

FIGURE 3 Detection of NLuc reporter signal in cells after IVT-CoV2-Rep RNA transfection. (A) Vero, (B,F) CHO-K1, (C) Huh7.5, and (D,E) BHK-21 cells were transfected with 200 ng IVT-CoV2-Rep RNA or N IVT RNA in a 96-well plate. NLuc activities were measured at indicated time points and plotted as relative luminescence units (RLU) (mean \pm SD, $n = 2$). IVT, in vitro transcription

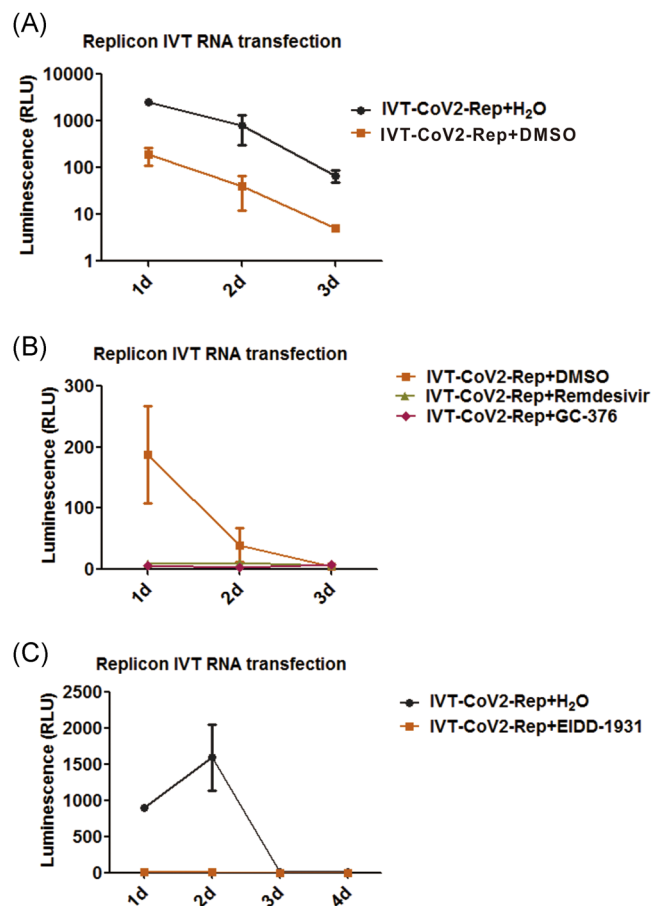


FIGURE 4 Inhibition of IVT-CoV2-Rep by antiviral compounds. CHO-K1 cells were transfected with 200 ng IVT-CoV2-Rep RNA in a 96-well plate and subjected to the following treatments: (A) Solvent control (0.1% DMSO or H₂O); (B) 5 μ M remdesivir or GC376 with DMSO as a control; and (C) 5 μ M EIDD-1931 with H₂O as a control. NLuc activities were measured at indicated time points (mean \pm SD, $n = 2$). DMSO, dimethyl sulfoxide; IVT, in vitro transcription; RLU, relative luminescence unit

(Figure 4A). The reason is not known, but perhaps is due to unexplained effects of DMSO on host cells.³⁶ Nonetheless, the compound test results demonstrated that all three SARS-CoV-2 replication inhibitors completely inhibited the NLuc activity in CHO-K1 cells transfected with IVT-CoV2-Rep mRNA (Figure 4B,C), which further confirmed that the IVT-CoV2-Rep-derived NLuc activity is replicon replication-dependent.

3.4 | Transient replicon replication is not due to host antiviral innate defense

It has been reported that the cellular pattern recognition receptor RIG-I/MDA5 can sense SARS-CoV-2 double stranded RNA (dsRNA) structures to induce type I/III IFNs, but the virus is able to antagonize the induction of IFNs and subsequent IFN-mediated Janus kinase-signal transducer and activator of transcription antiviral

signaling by a battery of viral nonstructural, structural, and accessory proteins.^{37–40} In light of the fact that IVT-CoV2-Rep does not encode viral structural and accessory proteins, we speculated that the transfected replicon RNA and/or replication intermediates might induce cellular innate immunity which eliminates replicon replication. However, it is also worth noting that among the above tested host cell lines, Huh7.5 possesses a mutationally inactivated RIG-I for IFN production,⁴¹ Vero cells lack the IFN- β gene,^{42,43} and BHK-21 cells have a compromised IFN induction and response,^{44–46} indicating that IFN may not be the culprit for the transient replicon replication. To further assess this possibility, we compared the inducibility of IFN- β by IVT-CoV2-Rep mRNA and an RIG-I agonist 3p-hpRNA in the IFN-competent CHO-K1 cells. First, we developed an RT-qPCR assay for detecting Chinese hamster IFN- β mRNA. The specificity of designed qPCR primers for IFN- β and GAPDH gene was confirmed by CHO-K1 cell genomic DNA PCR and mRNA RT-PCR (Figure S5). Transfection of 3p-hpRNA significantly induced IFN- β mRNA in CHO-K1 cells, while IVT-CoV2-Rep only slightly upregulated IFN- β compared to mock transfection. Interestingly, IVT-CoV2-Rep mRNA attenuated 3p-hpRNA-mediated IFN- β induction, indicating that the IVT-CoV-Rep inhibited the activation of innate signaling (Figure 5A). The above results are consistent with previous reports that SARS-CoV-2 NSPs antagonize IFN production.³⁷ However, the cotransfection of 3p-hpRNA still inhibited replicon replication to a great extent (Figure 5B), indicating that there may be an IFN-independent innate antiviral mechanism(s) upon 3p-hpRNA stimulation.

Next, we tested the possible effect of other two viral dsRNA-mediated innate antiviral mechanisms on shaping the transient phenotype of IVT-CoV2-Rep, specifically the PKR and oligoadenylate synthetase-RNase L.^{47,48} We first used compound C16, an inhibitor of PKR,^{49,50} to treat the CHO-K1 cells transfected with IVT-CoV2-Rep mRNA. The result demonstrated that C16 treatment increased replicon replication at day 1 posttransfection compared to DMSO control, but this pro-viral effect disappeared quickly by Day 2 (Figure 5C). Furthermore, we tested IVT-CoV2-Rep mRNA in A549DKO cells, a PKR and RNase L double knockout cell line.²⁷ Nevertheless, the replicon replication remained transient (Figure 5D). Collectively, these results suggested that the cellular innate immunity was not the major determinant of the unsustainable IVT-CoV2-rep replication.

3.5 | Characterization of BAC-CoV2-Rep

Another plausible explanation for the transient IVT-CoV2-Rep replication might be the low level of full-length IVT mRNA generated for transfection (Figure S2 and Table S2). We, therefore, set out to make use of the pCC1BAC vector system for transcription of the replicon mRNA in cells (Figures 1 and 2). To this end, the constructed BAC-CoV2-Rep was transfected into CHO-K1 cells with or without pcDNA6B-N, the N protein expressing vector. The transfection of BAC-CoV2-Rep produced strong NLuc signal, and the cotransfection of N protein further enhanced the signal level by more than fourfold

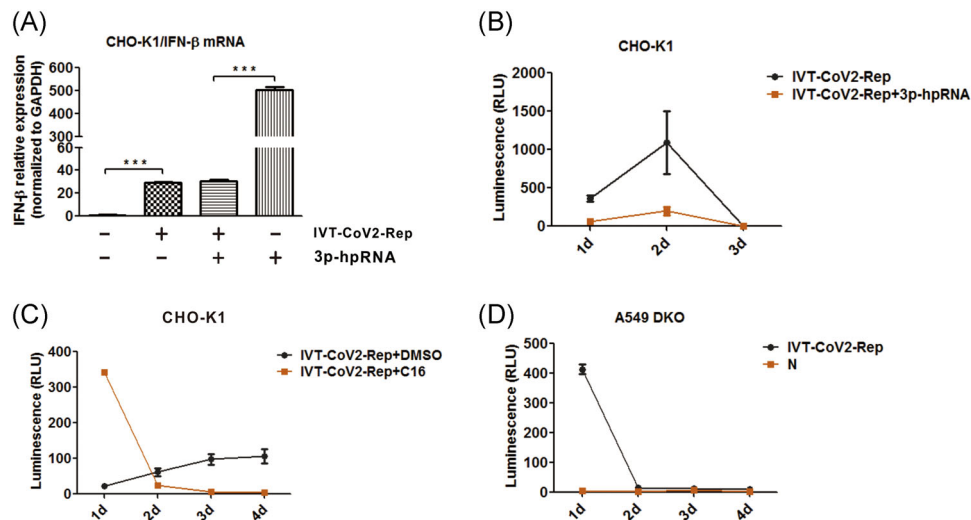


FIGURE 5 IVT-CoV2-Rep replication and cellular innate responses. (A) CHO-K1 cells were left untransfected or transfected with IVT-CoV2-Rep only, IVT-CoV2-Rep + 3p-hpRNA, or 3p-hpRNA only. The cells were harvested 2 days later for total RNA extraction, followed by RT-qPCR quantification of Chinese hamster IFN- β and GAPDH mRNAs. The relative expression levels of IFN- β mRNA compared to the untransfected control (set as 1) were normalized to GAPDH mRNA levels (mean \pm SD, $n = 3$; *** $p < 0.001$). (B) CHO-K1 cells were transfected with IVT-CoV2-Rep with or without 3p-hpRNA. NLuc activity was monitored daily for 3 days (mean \pm SD, $n = 2$). (C) CHO-K1 cells were transfected with IVT-CoV2-Rep and simultaneously treated with PKR inhibitor C16 (1 μ M). The NLuc activity was measured daily for 4 days (mean \pm SD, $n = 2$). (D) A549 DKO cells were transfected with IVT-CoV2-Rep or N mRNA. NLuc activity was measured daily for 4 days (mean \pm SD, $n = 2$). GAPDH, glyceraldehyde 3-phosphate dehydrogenase; hpRNA, hairpin RNA; IFN- β , interferon β ; IVT, in vitro transcription; mRNA, messenger RNA; RLU, relative luminescence unit; RT-qPCR, reverse transcription-quantitative polymerase chain reaction

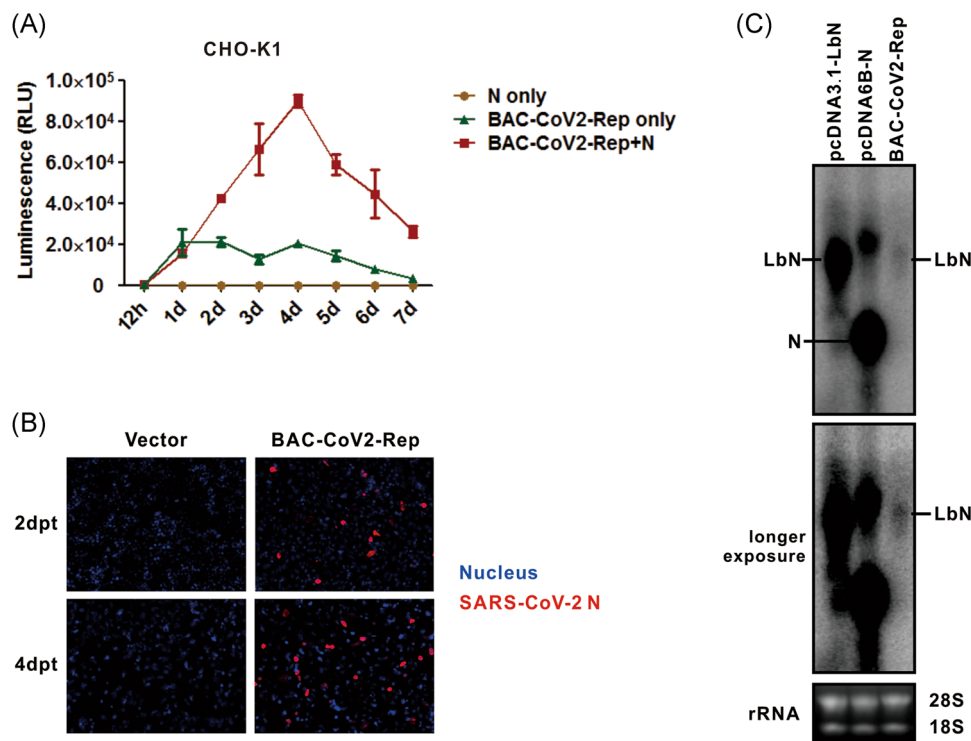


FIGURE 6 Replication of BAC-CoV2-Rep in cell culture. (A) CHO-K1 cells were transfected with the indicated plasmids. NLuc activity was measured at indicated time points and plotted as RLU (mean \pm SD, $n = 2$). (B) CHO-K1 cells were transfected with control vector or BAC-CoV2-Rep. At 2 and 4 days posttransfection, the N protein was detected in the cells by immunofluorescence using a SARS-CoV-2 N protein-specific antibody. (C) CHO-K1 cells were transfected with the indicated plasmids for 2 days. The total intracellular RNA was analyzed by Northern blot using an N gene sense strand-specific riboprobe. Ribosomal RNA (rRNA) served as a loading control. BAC, bacterial artificial chromosome; RLU, relative luminescence unit; SARS-CoV-2, severe acute respiratory syndrome coronavirus 2

at Day 4 posttransfection; though the signal started to decline after reaching a peak at Day 4, it remained detectable at Day 7, the end-point of the experiment (Figure 6A). Moreover, transfection of BAC-CoV2-Rep alone resulted in detection of N protein by immunofluorescence microscopy (Figure 6B). We also performed Northern blot analysis to detect the RNA species produced by BAC-CoV2-Rep. We found that the LbN mRNA could be detected at a low level, although the full-length replicon RNA and N mRNA were undetectable (Figure 6C). Altogether, these data demonstrated that the BAC-CoV2-Rep system is superior to the IVT-CoV2-Rep version with respect to reporter signal strength and duration, as well as viral subgenomic mRNA transcription and gene expression.

3.6 | The effect of antiviral drugs on BAC-CoV2-Rep

The BAC-CoV2-Rep-transfected CHO-K1 cells were treated with the same set of antiviral compounds used in the above IVT-CoV2-Rep experiment. However, the reduction of BAC-CoV2-Rep NLuc activity by antiviral treatment was not as significant as that observed in treatment of IVT-CoV2-Rep. Remdesivir only slightly reduced the NLuc level by ~10% (Figure 7A), which is somewhat consistent with a recent study using a similar BAC replicon system.²⁵ GC376 and EIDD-1931 decreased the NLuc signal by approximately 15% and 50%, respectively (Figure 7A). Interestingly, in Northern blot assay, the compounds exhibited a much stronger (~70-80%) inhibition of LbN mRNA synthesis (Figure 7B). The data indicated that the BAC-CoV2-Rep NLuc signal may not come exclusively from the LbN mRNA, which is in contrast to the IVT-CoV2-Rep system (Figure 4B,C). We then treated the BAC-CoV2-Rep-transfected CHO-K1 cells with blasticidin for 8 days. The selected cells were pooled and treated with Remdesivir or GC376. Under this condition, the NLuc signal was inhibited by ~70% (Figure 7C), indicating that the NLuc signal became more replication-dependent in the late phase of BAC-CoV2-Rep transfection.

3.7 | BAC-CoV2-Rep NLuc signal is partially derived from the spliced replicon mRNA

Considering that the NLuc signal in BAC-CoV2-Rep transfection might come from other sources independent of replicon replication, we speculated that this may be due to mRNA splicing since the initial replicon mRNA is transcribed from BAC-CoV2-Rep plasmid DNA in the cell nucleus, where RNA splicing occurs to transform pre-mRNAs into the mature mRNAs and to generate multiple functional mRNAs or proteins from a single transcript.⁵¹ To test this hypothesis, we designed a pair of primers targeting the 5' untranslated region (UTR) and Lb ORF on the replicon genome to detect potential spliced RNA species that could directly translate Lb (Figure 8A). Next, CHO-K1 cells were transfected with BAC-CoV2-Rep or the negative control pcDNA3.1-LbN, and total

RNA were extracted and subjected to RT-PCR. As shown in Figure 8B, RT-PCR with the N qPCR primers (Table S1) served as a positive control for the RT reaction (Lanes 2 and 3); the 21.8 kb PCR product from BAC-CoV2-Rep plasmid confirmed that the

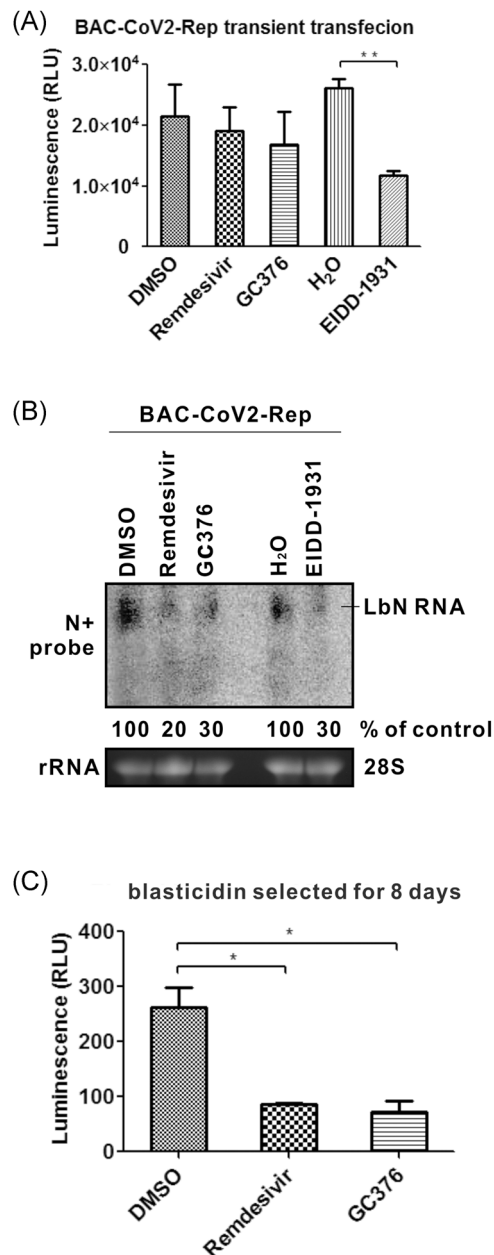


FIGURE 7 Antiviral treatment of BAC-CoV2-Rep replication. CHO-K1 cells were transfected with BAC-CoV2-Rep, followed by treatment with 10 μ M remdesivir, GC376, or EIDD-1931. 0.1% DMSO or H₂O served as solvent treatment control. After treatment for 2 days, cells were subjected to (A) an NLuc assay (mean \pm SD, $n = 2$; ** $p < 0.01$) and (B) a viral RNA Northern blot assay. (C) CHO-K1 cells were transfected with BAC-CoV2-Rep for 2 days, followed by blasticidin treatment (10 μ g/ml) for 8 days. The surviving cells were pooled and treated with remdesivir (10 μ M), GC376 (10 μ M), or DMSO control for 2 days. The treated cells were lysed and subjected to NLuc assay (mean \pm SD, $n = 2$; * $p < 0.05$). BAC, bacterial artificial chromosome; CMV, cytomegalovirus; DMSO, dimethyl sulfoxide; RLU, relative luminescence unit; rRNA, ribosomal RNA

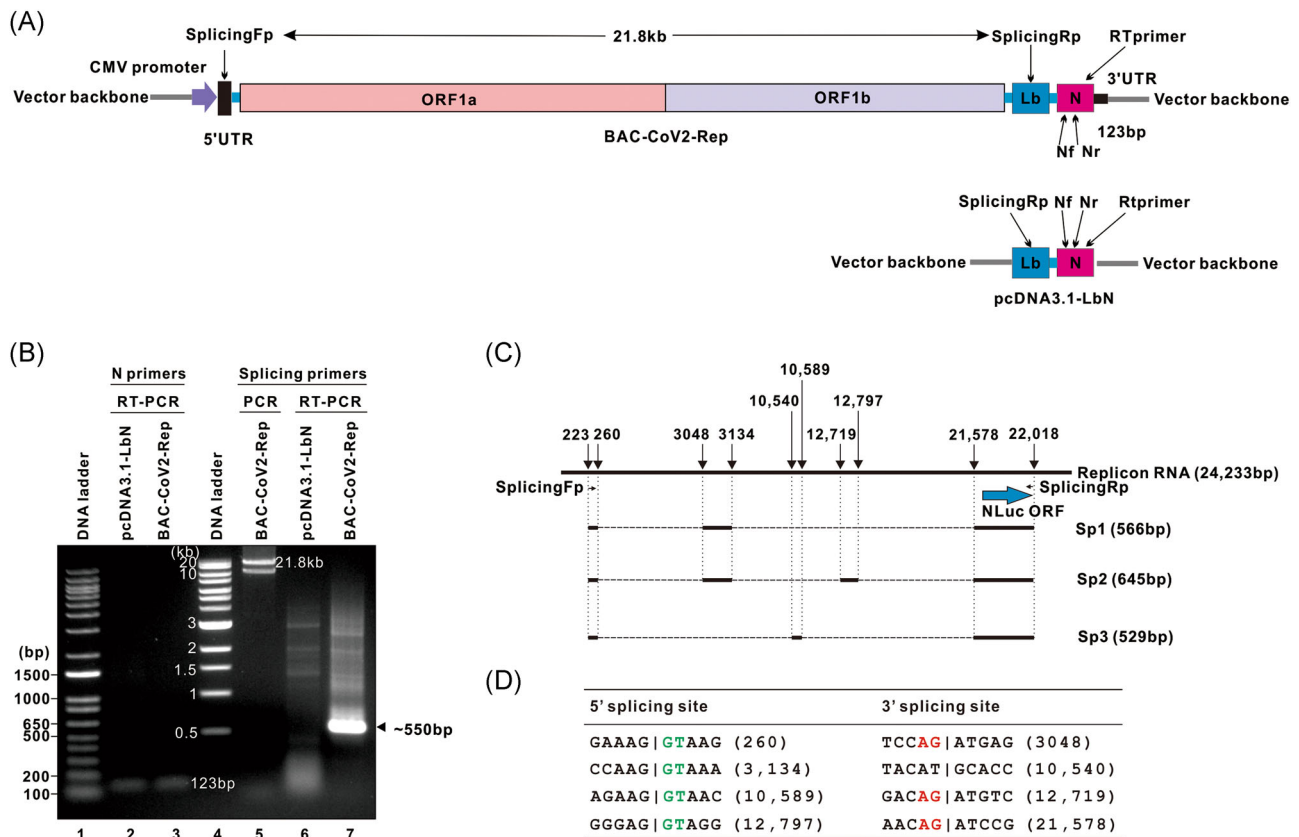


FIGURE 8 Identification of alternative splicing products of BAC-CoV2-Rep RNA. (A) A schematic design of RT-PCR detection of spliced replicon RNA is shown. The forward primer (Fp) targets an immediate downstream region of 5'UTR, the reverse primer (Rp) targets an internal sequence of Lb ORF. Nf and Nr are the primers for qPCR of N gene. The reverse transcription primer (Rtprimer) targets the 3' end of N ORF. The primer sequences are listed in Table S1. (B) CHO-K1 cells were transfected with pcDNA3.1-LbN or BAC-CoV2-Rep for 2 days. Total RNA was extracted from the transfected cells and subjected to RT-PCR using the indicated primers, followed by agarose gel analysis. RT-PCR by N primers and direct PCR of BAC-CoV2-Rep by splicing primers were used to validate the RT reaction and primer design. A predominant BAC-CoV2-Rep-derived RT-PCR product of ~550 bp is indicated by a triangle symbol. (C) The ~550 bp RT-PCR product was gel purified, cloned into vector, and sequenced. Three detected splicing variants of BAC-CoV2-Rep RNA, specifically Sp1, Sp2, and Sp3, are schematically illustrated underneath the full-length replicon. The numbers indicate the nucleotide positions of splicing sites. (D) The sequences of identified 5' and 3' splicing sites are listed. The consensus sequences of canonical 5' splice donor and 3' acceptor motif GT_{AG} are in green and red color, respectively. BAC, bacterial artificial chromosome; CMV, cytomegalovirus; ORF, open reading frame; RT-qPCR, reverse transcription-quantitative polymerase chain reaction; UTR, untranslated region

splicing primers worked (Lane 5). Comparing the total RNA RT-PCR products from cells transfected with pcDNA3.1-LbN and BAC-CoV2-Rep, a predominant band of ~550 bp in the BAC-CoV2-Rep sample was observed (Lane 7), despite the detection of additional faint background bands in both samples (Lanes 6 and 7).

The ~550 bp band was then gel purified and cloned into a plasmid for sequencing. After sequencing more than 20 clones, three major splicing RNA species were identified and their splicing sites are described in Figure 8C. Sp1, Sp2, and Sp3 all possess the sequence of NLuc ORF with a variable short 5' untranslated region. The sequences at the identified splicing sites are consistent with the major splice donor and acceptor consensus motif "GT_{AG}," and there is only one noncanonical 3' acceptor sequence (Figure 8D).⁵² Taken together, the data demonstrate that BAC-CoV2-Rep mRNA splicing occurs during transient transfection, giving rise to cryptic NLuc reporter signals independent of replicon replication.

4 | DISCUSSION

Reverse genetics-based viral replicon systems have significantly contributed to virus research, especially for the single-stranded positive RNA viruses, such as HCV and other flaviviruses (Dengue, ZIKA), picornaviruses (Polio, hepatitis A virus), caliciviruses (Norovirus, hepatitis E virus), alphaviruses (Chikungunya virus), and coronaviruses (SARS, Middle East respiratory syndrome).⁵³ The viral subgenomic replicons comprising nonstructural genes essential to viral RNA replication but without structural genes are convenient tools when in vitro infection systems are unavailable or downgrade of biosafety levels is needed. In addition, reporter genes can be engineered into replicons for high sensitivity and ease of detection, especially for high throughput antiviral screening purposes.⁵⁴ Compared to in vitro enzymatic assay-based antiviral screening platforms, a replicon system is advantageous in the assessment of compound cytotoxicity and

combination treatments, selection of drug resistant mutants, and discovery and evaluation of host targeting antiviral agents.

Reverse genetics approaches were used to generate SARS-CoV-2 infectious clone and replicon systems immediately after the whole viral genome sequence became publicly available.^{24,40} Due to the large size of SARS-CoV-2 genome, the viral cDNA genome was designed as split fragments of ~5 kb each with suitable type IIS restriction sites located at the junctions, then the chemically synthesized fragments were subjected to restriction enzyme digestion and ligated into cDNA *in vitro*.^{23,37} In addition, a prokaryotic promoter sequence, such as T7, and a poly(A) sequence were typically placed at the 5' and 3' termini of the replicon cDNA, respectively. To rapidly acquire the replicon mRNA, most researchers performed IVT of the assembled replicon cDNA.^{20,40} Alternatively, others further cloned the aforementioned cDNA into BAC vectors to obtain a more consistent and scalable production of replicon cDNA template for IVT.^{19,23,25} It is worth noting that the above reverse genetics approaches have been successfully used previously in generating other coronavirus replicons.⁵⁵ A recent study employed the TAR apparatus to assemble large overlapping SARS-CoV-2 cDNA fragments to create a replicon DNA plasmid in the yeast *Saccharomyces cerevisiae*.^{22,56} Another group reported a SARS-CoV-2 replicon transfection system consisting of four plasmids expressing ORF1ab proteins and the minimally required viral segments *in trans*.²¹ Among the designs of aforementioned replicons, different viral structural and accessory genes were omitted and different reporter genes were used. In all the cases, S gene was deleted to prevent infectious virus production. Bioluminescence or fluorescence proteins, such as luciferase and GFP, were commonly chosen as reporters to facilitate the detection and standardization of the replicon systems. Furthermore, to select the stable replicon in cells, antibiotic-resistant genes, such as NeoR or BSR, were incorporated into the replicons.^{17,53}

In this study, we designed a subgenome of SARS-CoV-2 by omitting structural genes S, E, M, and all the accessory genes except for the 5' and 3' UTR, ORF1ab, and N sequence (Figure 1). This is the minimum version of a replicon that has been proven to work for SARS-CoV-1.¹⁸ We used NLuc as reporter gene to monitor the replicon replication level. A BSR ORF was fused to the NLuc gene with a short linker in between and the fused protein was named Lb. We confirmed that the Lb fusion protein maintains both NLuc and BSR functions (Figure S1 and data not shown). The N protein is known to be important for the replication of coronaviruses.³² We thus included the N ORF and its 5' TRS-N sequence downstream of the Lb fusion gene. The full-length replicon cDNA was assembled by *in vitro* ligation of the synthetic fragments (Figures 1 and 2), which was subjected to replicon RNA production *in vitro* and in cells.

First, we took advantage of the pre-engineered T7 promoter at the 5' terminus of F1 to produce IVT mRNA using the IVT-CoV2-Rep cDNA template directly (Figure 2C,D). The IVT-CoV2-Rep mRNA rapidly produced NLuc reporter signals upon transfection into host cells, which could be completely abolished by SARS-CoV-2 replication inhibitors. This result suggested that the replicon mRNA is able to initiate replication by at least the production of subgenomic RNAs

(Figures 3 and 4). However, the NLuc signal was rather weak and transitory in various cell lines tested, indicating that the replicon RNA replication is self-limiting or there is a host mechanism restricting the replicon. Considering that the transfected IVT-CoV2-Reported mRNA may act as a pathogen-associated molecular pattern to activate a cellular innate antiviral response, we thus examined whether innate immunity was responsible for the transient replicon replication. While the known deficiency of IFN signaling or response in Huh7.5, Vero, and BHK-21 cells does not support this possibility,⁴¹⁻⁴⁶ we have obtained further evidence that the IVT-CoV2-Rep RNA fails to induce IFN- β in CHO-K1 cells but it attenuates 3p-hpRNA-elicited IFN- β expression (Figure 5A). This is consistent with reported findings that SARS-CoV-2 evades type I IFN via antagonizing IFN signaling and response by a set of viral proteins.^{38,40} Furthermore, we have ruled out the potential role of two dsRNA-activated antiviral proteins, specifically PKR and RNase L, in restricting the replicon RNA (Figure 5C,D). Taken together, these data suggested that the host cell innate immunity may not be the major cause for the unsustainability of replicon RNA.

The transient replicon RNA replication might be due to the inadequate yield of full-length IVT-CoV2-Rep mRNA for transfection (Figure S2, Table S2). Therefore, we constructed the DNA-launched BAC-CoV2-Rep replicon, which expresses the full-length replicon mRNA in transfected cells by employing the robust CMV promoter and cellular transcription machinery. Indeed, BAC-CoV2-Rep exhibited a much stronger and sustained NLuc signal than IVT-CoV2-Rep, and addition of the N protein could further enhance the replicon reporter signal *in trans*, although replicon replication declined over time after it reached the peak level (Figure 6A). The N protein expressed from the replicon could also be detected (Figure 6B). In addition, the LbN mRNA was detected by Northern blot as a reliable indicator of BAC-CoV2-Rep replication (Figure 6C). The antiviral compounds markedly suppressed LbN RNA level by more than 70% (Figure 7B), however, the NLuc signal was only slightly inhibited when the treatment started immediately after BAC-CoV2-Rep transfection (Figure 7A). A recent study of another pBAC-launched replicon system also reported such resistance to drug treatment but did not provide further explanation.²⁵ In our study, we showed that a portion of BAC-CoV2-Rep full-length transcripts undergo long-range RNA splicing upstream of Lb ORF, which brings the Lb ORF in close proximity to 5' Cap for Lb translation in a replicon replication-independent manner (Figure 8). We identified three forms of spliced replicon RNA by RT-PCR with primers targeting 5' UTR and Lb sequence (Figure 8). Although we only sequenced a limited number of RT-PCR clones for proof-of-concept in this study, it is expected that additional splicing variants exist in BAC-CoV2-Rep-transfected cells, which can be analyzed further by RNA sequencing. The splicing of replicon RNA transcribed from BAC-CoV2-Rep may also explain the undetectable level of full-length replicon RNA by Northern blot (Figure 6C). Interestingly, during the late phase of BAC-CoV2-Rep transfection, the NLuc reporter was more vulnerable to antiviral treatment (Figure 7C), which may be due to the dilution, degradation, or epigenetic silencing of the BAC-CoV2-Rep episome as seen in

transient DNA transfection systems,⁵⁷ or the cellular spliceosome is inhibited by viral NSP16 protein upon expression,⁵⁸ therefore, the replicon replication-derived reporter signal becomes predominant in the system. It is worth noting that the observed SARS-CoV-2 RNA splicing is likely specific to the DNA-launched replicon systems, and it should be taken into consideration for its applications in research and development.

While the full-length SARS-CoV-2 cDNA clone exhibited robust viral replication and spread, all the reported SARS-CoV-2 subgenome replicon systems, so far, as well as the replicons described in this study, only supported transient replicon replication. Since our replicons only contain the minimum elements needed for viral genome replication, it is possible that transcomplementing the missing viral proteins may boost and prolong the replicon replication. In line with this, a recently published study, in which only S, E, and M ORF were omitted in their replicon construct, showed a drastic reduction of replication reporter signal after day 2 posttransfection.¹⁹ We have tested cotransfection of IVT-CoV2-Rep mRNA together with different combinations of plasmids expressing viral structural proteins (not S) and accessory proteins, but did not observe any obvious improvement of replicon replication (data not shown). More recently, a SARS-CoV-2 replicon having all viral sequence except for the S ORF also exhibited a decreasing trend of replication after 2 day post-transfection, however, when S was provided *in trans*, the produced propagation-defective recombinant virus still lost ~25% infectivity and replication compared to the wild type virus.²² These results suggest that, in addition to viral proteins, there may be *cis* elements in S gene and other regions between ORF1b and N gene that could assist a sustained replication of SARS-CoV-2 genome. It is also possible that the engineered reporter and/or antibiotics-resistant gene sequences may negatively affect replicon replication. On a separate note, it has been reported that SARS-CoV-2 NSP1 is a cytotoxic protein that can shut down host cell translation,⁵⁹ which may affect the cell viability of replicon-containing cells and eventually halt replicon replication. However, no cytotoxicity was observed in our replicon systems (data not shown), and a reported replicon harboring non-cytopathic NSP1 mutation failed to form stable replicon cell clones.²² Therefore, to generate a stable SARS-CoV-2 replicon, the architecture of replicon should be further rearranged and optimized to include all necessary genes and *cis* elements required for viral replication.

Regarding the BAC-CoV2-Rep system, a further optimization effort could be the elimination of RNA splicing through mutating the splicing donor or acceptor sites. By doing this, more full-length replicon mRNA and RTC would be available to subsequent rounds of replication and replication-dependent reporter production. Furthermore, the BAC-CoV2-Rep holds promise for establishing stable replicon cell lines through blasticidin selection of cells harboring self-replicating replicons. Alternatively, a stable replicating BAC-CoV2-Rep plasmid may be constructed by incorporating the Epstein-Barr virus nuclear antigen-1 its binding oriP DNA sequence,⁶⁰ or the replicon DNA cassette can be integrated into host

chromosome, by which to serve as a source for stable production of replicon mRNA. In either case, N protein can be stably co-expressed to enhance and prolong the replicon replication. The above proposed work is currently under way in our laboratory.

In summary, we have established two transient minigenome replicons that can be readily applied to research on SARS-CoV-2 replication, virus-host interaction, and antiviral development. This study will also advance the ultimate development of stable SARS-CoV-2 replicon systems amenable to high throughput screening of antiviral drugs to combat the coronavirus pandemic.

ACKNOWLEDGMENTS

This study was supported by the University of Pittsburgh Medical Center Hillman Cancer Center Startup Fund (to Haitao Guo) and COVID-19 Pilot Program award from the University of Pittsburgh Clinical and Translational Science Institute and the DSF Charitable Foundation (to Zandrea Ambrose). Patrick S. Moore is supported as a Pittsburgh Foundation Professor for Innovative Cancer Research. The authors would like to thank Drs. Pei-Yong Shi (University of Texas Medical Branch), Paul Duprex (University of Pittsburgh Center for Vaccine Research), Pei-Hui Wang (Shandong University), Yuan Liu (Cornell University), Robert Campbell (University of Alberta), Bernard Moss (NIAID/NIH), and Charles Rice (Rockefeller University) for generously providing reagents for this study. They would also like to thank Dr. Yuan Chang (University of Pittsburgh) for critical reading of the manuscript.

CONFLICT OF INTERESTS

The authors declare no conflict of interests.

AUTHOR CONTRIBUTIONS

Conceptualization, plan, and management: Haitao Guo. *Experimental design:* Hu Zhang, Douglas K. Fischer, Zandrea Ambrose, and Haitao Guo. *Execution of experiments, acquisition, analysis, or interpretation of data:* Hu Zhang, Douglas K. Fischer, Masahiro Shuda, Patrick S. Moore, Shou-Jiang Gao, Zandrea Ambrose, and Haitao Guo. *Drafting and revision of the manuscript:* Hu Zhang and Haitao Guo. *Manuscript editing and approval:* Hu Zhang, Douglas K. Fischer, Masahiro Shuda, Patrick S. Moore, Shou-Jiang Gao, Zandrea Ambrose, and Haitao Guo.

DATA AVAILABILITY STATEMENT

The data that support the findings of this study are available on request from the corresponding author. The data are not publicly available due to privacy or ethical restrictions.

ORCID

Shou-Jiang Gao  <http://orcid.org/0000-0001-6194-1742>

Haitao Guo  <http://orcid.org/0000-0002-7146-916X>

PEER REVIEW

The peer review history for this article is available at <https://publons.com/publon/10.1002/jmv.27650>

REFERENCES

- Zhou P, Yang XL, Wang XG, et al. A pneumonia outbreak associated with a new coronavirus of probable bat origin. *Nature*. 2020;579(7798):270-273.
- Wu F, Zhao S, Yu B, et al. A new coronavirus associated with human respiratory disease in China. *Nature*. 2020;579(7798):265-269.
- Coronaviridae Study Group of the International Committee on Taxonomy of Viruses. The species *Severe acute respiratory syndrome-related coronavirus*: classifying 2019-nCoV and naming it SARS-CoV-2. *Nat Microbiol*. 2020;5:536-544.
- Harvey WT, Carabelli AM, Jackson B, et al. SARS-CoV-2 variants, spike mutations and immune escape. *Nat Rev Microbiol*. 2021;19(7):409-424.
- Gao SJ, Guo H, Luo G. Omicron variant (B.1.1.529) of SARS-CoV-2, a global urgent public health alert! *J Med Virol*. 2021.
- Hu B, Guo H, Zhou P, Shi ZL. Characteristics of SARS-CoV-2 and COVID-19. *Nat Rev Microbiol*. 2021;19(3):141-154.
- Wu A, Peng Y, Huang B, et al. Genome composition and divergence of the novel coronavirus (2019-nCoV) originating in China. *Cell Host Microbe*. 2020;27(3):325-328.
- Kelly JA, Woodside MT, Dinman JD. Programmed-1 ribosomal frameshifting in coronaviruses: a therapeutic target. *Virology*. 2021;554:75-82.
- Chen Y, Liu Q, Guo D. Emerging coronaviruses: genome structure, replication, and pathogenesis. *J Med Virol*. 2020;92(10):2249.
- V'kovski P, Kratzel A, Steiner S, Stalder H, Thiel V. Coronavirus biology and replication: implications for SARS-CoV-2. *Nat Rev Microbiol*. 2021;19(3):155-170.
- Sola I, Almazan F, Zuniga S, Enjuanes L. Continuous and discontinuous RNA synthesis in coronaviruses. *Annu Rev Virol*. 2015;2(1):265-288.
- Hartenian E, Nandakumar D, Lari A, Ly M, Tucker JM, Glaunsinger BA. The molecular virology of coronaviruses. *J Biol Chem*. 2020;295(37):12910-12934.
- Brant AC, Tian W, Majerciak V, Yang W, Zheng ZM. SARS-CoV-2: from its discovery to genome structure, transcription, and replication. *Cell Biosci*. 2021;11(1):136.
- Schafer A, Baric RS, Ferris MT. Systems approaches to Coronavirus pathogenesis. *Curr Opin Virol*. 2014;6:61-69.
- Xie X, Lokugamage KG, Zhang X, et al. Engineering SARS-CoV-2 using a reverse genetic system. *Nat Protoc*. 2021;16(3):1761-1784.
- Pietschmann T, Bartenschlager R. The hepatitis C virus replicon system and its application to molecular studies. *Curr Opin Drug Discov Devel*. 2001;4(5):657-664.
- Hannemann H. Viral replicons as valuable tools for drug discovery. *Drug Discovery Today*. 2020;25(6):1026-1033.
- Ge F, Luo Y, Liew PX, Hung E. Derivation of a novel SARS-coronavirus replicon cell line and its application for anti-SARS drug screening. *Virology*. 2007;360(1):150-158.
- He X, Quan S, Xu M, et al. Generation of SARS-CoV-2 reporter replicon for high-throughput antiviral screening and testing. *Proc Natl Acad Sci U S A*. 2021;118(15):e2025866118.
- Kotaki T, Xie X, Shi P-Y, Kameoka MA. PCR amplicon-based SARS-CoV-2 replicon for antiviral evaluation. *Sci Rep*. 2021;11(1):2229.
- Luo Y, Yu F, Zhou M, et al. Engineering a reliable and convenient SARS-CoV-2 replicon system for analysis of viral RNA synthesis and screening of antiviral inhibitors. *mBio*. 2021;12(1):e02754.
- Ricardo-Lax I, Luna JM, Thao TTN, et al. Replication and single-cycle delivery of SARS-CoV-2 replicons. *Science*. 2021;374(6571):1099-1106.
- Zhang Y, Song W, Chen S, Yuan Z, Yi Z. A bacterial artificial chromosome (BAC)-vectored noninfectious replicon of SARS-CoV-2. *Antiviral Res*. 2021;185:104974.
- Xie X, Muruato A, Lokugamage KG, et al. An infectious cDNA Clone of SARS-CoV-2. *Cell Host Microbe*. 2020;27(5):841-848.
- Nguyen HT, Falzarano D, Gerdt V, Liu Q. Construction of a non-infectious SARS-CoV-2 replicon for antiviral-drug testing and gene function studies. *J Virol*. 2021;95(18):e0068721.
- Blight KJ, McKeating JA, Rice CM. Highly permissive cell lines for subgenomic and genomic hepatitis C virus RNA replication. *J Virol*. 2002;76(24):13001-13014.
- Liu R, Moss B. Opposing roles of double-stranded RNA effector pathways and viral defense proteins revealed with CRISPR-Cas9 knockout cell lines and vaccinia virus mutants. *J Virol*. 2016;90(17):7864-7879.
- Zhang W, Lohman AW, Zhuravlova Y, et al. Optogenetic control with a photocleavable protein, PhoCl. *Nat Methods*. 2017;14(4):391-394.
- Zhang J, Cruz-Cosme R, Zhuang MW, et al. A systemic and molecular study of subcellular localization of SARS-CoV-2 proteins. *Signal Transduct Target Ther*. 2020;5(1):269.
- Wild J, Hradecna Z, Szybalski W. Conditionally amplifiable BACs: switching from single-copy to high-copy vectors and genomic clones. *Genome Res*. 2002;12(9):1434-1444.
- Cai D, Nie H, Yan R, Guo JT, Block TM, Guo H. A southern blot assay for detection of hepatitis B virus covalently closed circular DNA from cell cultures. *Methods Mol Biol*. 2013;1030:151-161.
- Almazán F, Galán C, Enjuanes L. The nucleoprotein is required for efficient coronavirus genome replication. *J Virol*. 2004;78(22):12683-12688.
- Wang M, Cao R, Zhang L, et al. Remdesivir and chloroquine effectively inhibit the recently emerged novel coronavirus (2019-nCoV) in vitro. *Cell Res*. 2020;30(3):269-271.
- Rosenke K, Hansen F, Schwarz B, et al. Orally delivered MK-4482 inhibits SARS-CoV-2 replication in the Syrian hamster model. *Nat Commun*. 2021;12(1):2295.
- Fu L, Ye F, Feng Y, et al. Both Boceprevir and GC376 efficaciously inhibit SARS-CoV-2 by targeting its main protease. *Nat Commun*. 2020;11(1):4417.
- Cushnie TPT, Cushnie B, Echeverría J, et al. Bioprospecting for antibacterial drugs: a multidisciplinary perspective on natural product source material, bioassay selection and avoidable pitfalls. *Pharm Res*. 2020;37(7):125.
- Sa Ribero M, Jouvenet N, Dreux M, Nisole S. Interplay between SARS-CoV-2 and the type I interferon response. *PLoS Pathog*. 2020;16(7):e1008737.
- Kim YM, Shin EC. Type I and III interferon responses in SARS-CoV-2 infection. *Exp Mol Med*. 2021;53(5):750-760.
- Thorne LG, Reuschl AK, Zuliani-Alvarez L, et al. SARS-CoV-2 sensing by RIG-I and MDA5 links epithelial infection to macrophage inflammation. *EMBO J*. 2021;40(15):e107826.
- Xia H, Cao Z, Xie X, et al. Evasion of Type I Interferon by SARS-CoV-2. *Cell Rep*. 2020;33(1):108234.
- Sumpter R Jr., Loo YM, Foy E, et al. Regulating intracellular antiviral defense and permissiveness to hepatitis C virus RNA replication through a cellular RNA helicase, RIG-I. *J Virol*. 2005;79(5):2689-2699.
- Desmyter J, Melnick JL, Rawls WE. Defectiveness of interferon production and of rubella virus interference in a line of African green monkey kidney cells (Vero). *J Virol*. 1968;2(10):955-961.
- Mosca JD, Pitha PM. Transcriptional and posttranscriptional regulation of exogenous human beta interferon gene in simian cells defective in interferon synthesis. *Mol Cell Biol*. 1986;6(6):2279-2283.
- Habjan M, Penski N, Spiegel M, Weber F. T7 RNA polymerase-dependent and -independent systems for cDNA-based rescue of Rift Valley fever virus. *J Gen Virol*. 2008;89(Pt 9):2157-2166.
- Otsuki K, Maeda J, Yamamoto H, Tsubokura M. Studies on avian infectious bronchitis virus (IBV). III. Interferon induction by and sensitivity to interferon of IBV. *Arch Virol*. 1979;60(3-4):249-255.

46. Chinsangaram J, Piccone ME, Grubman MJ. Ability of foot-and-mouth disease virus to form plaques in cell culture is associated with suppression of alpha/beta interferon. *J Virol.* 1999;73(12):9891-9898.
47. Sadler AJ, Williams BR. Interferon-inducible antiviral effectors. *Nat Rev Immunol.* 2008;8(7):559-568.
48. Li Y, Renner DM, Comar CE, et al. SARS-CoV-2 induces double-stranded RNA-mediated innate immune responses in respiratory epithelial-derived cells and cardiomyocytes. *Proc Natl Acad Sci U S A.* 2021;118(16).
49. Jammi NV, Whitby LR, Beal PA. Small molecule inhibitors of the RNA-dependent protein kinase. *Biochem Biophys Res Commun.* 2003;308(1):50-57.
50. Watanabe T, Ninomiya H, Saitou T, et al. Therapeutic effects of the PKR inhibitor C16 suppressing tumor proliferation and angiogenesis in hepatocellular carcinoma in vitro and in vivo. *Sci Rep.* 2020;10(1):5133.
51. Sharp PA. The discovery of split genes and RNA splicing. *Trends Biochem Sci.* 2005;30(6):279-281.
52. Black DL. Mechanisms of alternative pre-messenger RNA splicing. *Annu Rev Biochem.* 2003;72:291-336.
53. Tews BA, Meyers G. Self-Replicating RNA. *Methods Mol Biol.* 2017;1499:15-35.
54. Fernandes RS, Freire M, Bueno RV, Godoy AS, Gil L, Oliva G. Reporter replicons for antiviral drug discovery against positive single-stranded RNA viruses. *Viruses.* 2020;12(6):598.
55. Almazan F, Sola I, Zuniga S, et al. Coronavirus reverse genetic systems: infectious clones and replicons. *Virus Res.* 2014;189:262-270.
56. Thi Nhu Thao T, Labroussaa F, Ebert N, et al. Rapid reconstruction of SARS-CoV-2 using a synthetic genomics platform. *Nature.* 2020;582(7813):561-565.
57. Kim TK, Eberwine JH. Mammalian cell transfection: the present and the future. *Anal Bioanal Chem.* 2010;397(8):3173-3178.
58. Banerjee AK, Blanco MR, Bruce EA, et al. SARS-CoV-2 disrupts splicing, translation, and protein trafficking to suppress host defenses. *Cell.* 2020;183(5):1325-1339.
59. Schubert K, Karousis ED, Jomaa A, et al. SARS-CoV-2 Nsp1 binds the ribosomal mRNA channel to inhibit translation. *Nat Struct Mol Biol.* 2020;27(10):959-966.
60. Yates JL, Warren N, Sugden B. Stable replication of plasmids derived from Epstein-Barr virus in various mammalian cells. *Nature.* 1985;313(6005):812-815.

SUPPORTING INFORMATION

Additional supporting information may be found in the online version of the article at the publisher's website.

How to cite this article: Zhang H, Fischer DK, Shuda M, et al. Construction and characterization of two SARS-CoV-2 minigenome replicon systems. *J Med Virol.* 2022;94:2438-2452. doi:10.1002/jmv.27650